

Current Distribution of Lead Ions Deposition Within Porous Flow-Through Electrodes Operating Under Simultaneous Hydrogen Gas Evolution

Mohamed S. El-Deab^{1,*}, Mohamed I. Awad^{1,2}, Aya Md. Saada³ and Attia M. Attia^{4,*}

¹ Chemistry Department, Faculty of Science, Cairo University, 12613 Cairo, Egypt

² Chemistry Department, Faculty of Applied Science, Umm Al-Qura University, Makkah, KSA

³ Biochemical Engineering Department, Faculty of Energy and Environmental Engineering, The British University in Egypt (BUE), El Shorouk City, 11837, Cairo, Egypt

⁴ Petroleum Engineering and Gas Technology Department, Faculty of Energy and Environmental Engineering, The British University in Egypt (BUE), El Shorouk City, 11837, Cairo, Egypt

*E-mail: msaada68@yahoo.com (M. S. El-Deab), attia.attia@bue.edu.eg (Attia M. Attia).

Received: 15 October 2020 / Accepted: 24 December 2020 / Published: 31 March 2021

This study addresses the impact of operating hydrodynamic and structural parameters affecting the distribution of metal deposition current within flow-through porous reactors, i.e., the electrolyte resistivity (ρ_{eff}) and flow rate (v) as well as the electrode thickness (L) of the porous bed. Measurements are performed on the distribution of the lead deposition reaction within packed bed electrodes composed of stacked screens, with simultaneous hydrogen evolution (as a parasitic side reaction). The uniformity of the current distribution is found to increase with the decrease of the electrolyte resistivity and/or increase of electrolyte flow rate, while increase of the electrode thickness results in a less uniform current distribution. The results are explained in the light of the existing electrochemical theory, in which a dimensionless ohmic index, ξ ($= i_{\text{cell}} \rho_{\text{eff}} L/b$ where i_{cell} is the cell current and $b = RT/F$) is developed. Larger values of ξ produce less uniform current distributions with less than 10% of the entire thickness of the porous bed is in effective use. Whereas, higher electrolyte flow rates sweeps away the generated gas bubbles, thus, causes a marked decrease of ρ_{eff} by decreasing the fraction of the trapped hydrogen gas bubbles within the electrode and hence lead to more uniform current distributions.

Keywords: Porous reactors, Gas evolving electrodes, Heavy metals, Wastewater treatment.

1. INTRODUCTION

Catalysis and electrocatalysis by 3D porous materials has been increasingly motivated in view of their several operational and structural virtues [1-10]. This includes the synthesis of metastable intermetallic electrocatalysts [11,12] for application in oxygen reduction reaction [12]. Also the

electrodeposition of highly porous Zn [13] and Zn-rich porous Zn-Cu based alloys [14] have been introduced as active materials for boosted CO₂ electroreduction [13] and as alternative anode materials for Li-ion batteries [14]. Of these, porous flow-through electrodes are promising category of 3D catalysts due to: (i) their high effective surface areas enclosed in fairly small volumes which enhances the cell house productivity, (ii) they allow for continuous rather than batch operations by forced convection of the electrolyte, and (iii) separating the reacted from the unreacted species while operating at 100% efficiency per pass. This system has been suggested for several applications including energy conversion, water electrolysis and wastewater treatment [14-20]. In this regard, several geometries of 3D catalysts are suggested as potential porous electrodes, including stacked screens, packed beds of fine particulates, porous metallic structures, metal foams, carbon felts as well as porous carbon (e.g., RVC), and active carbon [4,5, 18, 21-24]. The proper selection of the material and geometry of porous reactors are crucial parameters in determining its overall performance and efficacy for a target application [25,26].

Porous flow-through electrodes (PFTE) offer several operational advantages compared to planar electrodes or porous electrodes operating on stationary electrolytes [27-32]. However, under virtually all the experimental conditions, the reaction is non-uniformly distributed within the PFTE. Extensive modeling work was done on this system to predict the effect of various controlling parameters on the current distribution within the electrode [33-37]. Much work was done on this system using redox reactions where experimental measurements of current distributions [38-42] are difficult to achieve. On the other hand, some studies were performed on metal deposition reactions, e.g., Cu and Zn [37, 43-45] using electrodes which can be sectioned where the current distribution can be readily determined from weight changes.

The objective of this paper is to investigate the effects of structural and hydrodynamic operating parameters (i.e., electrode thickness, electrolyte resistivity and flow rate) on the current distributions of lead ions deposition from flowing alkaline electrolyte with simultaneous hydrogen gas evolution within PFTE. This is done with an aim to maximize the cell house productivity and maximize the removal efficiency of the polluting heavy metal ions (Pb²⁺) from the flowing streams.

2. EXPERIMENTAL

The porous electrodes are in the form of packed beds made up of several (pre-weighed) stacked screens (mesh size = 60 ppi, specific surface area = 74 cm⁻¹). Fig. 1 shows SEM image of a single screen. A number of screens are stacked in the electrode chamber and pressed tightly together to achieve the desired electrode thickness and to ensure excellent electrical contact between the bottom and the top most screens together with the current collector. Spiral Pt wire and Hg/HgO/KOH(1M) (having an equilibrium potential of 98 mV vs. NHE) are used as the counter and the reference electrodes, respectively. Fig. 2 shows a schematic diagram of the electrode chamber, the direction of electrolyte flow and the position of the reference and counter electrodes. The electrochemical measurements are carried out using alkaline electrolytes (1.0 and 3.0 M NaOH) containing 0.01 M lead ions. The electrolyte is forced from the bottom (entry) face of the porous electrode using a variable speed peristaltic pump (Manostat, USA). EG&G potentiostat (Model 273A) operated with chem253 software is used to perform

the electrochemical measurements. The current distribution of lead ions deposition is performed at a constant cell current density (i_{cell}) which is just at the rising part of the experimentally measured limiting current density. Fig. 3 shows a representative example of $i-E$ relations for lead ions deposition from aqueous alkaline NaOH electrolytes. Obviously, the limiting current of lead ions deposition depends on the supporting electrolyte concentration.

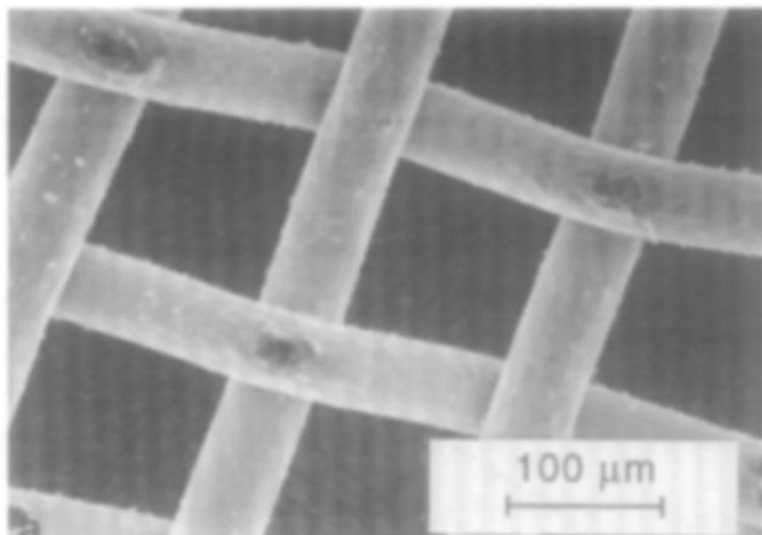


Figure 1. SEM image of a single Cu screen (mesh size = 60 ppi)

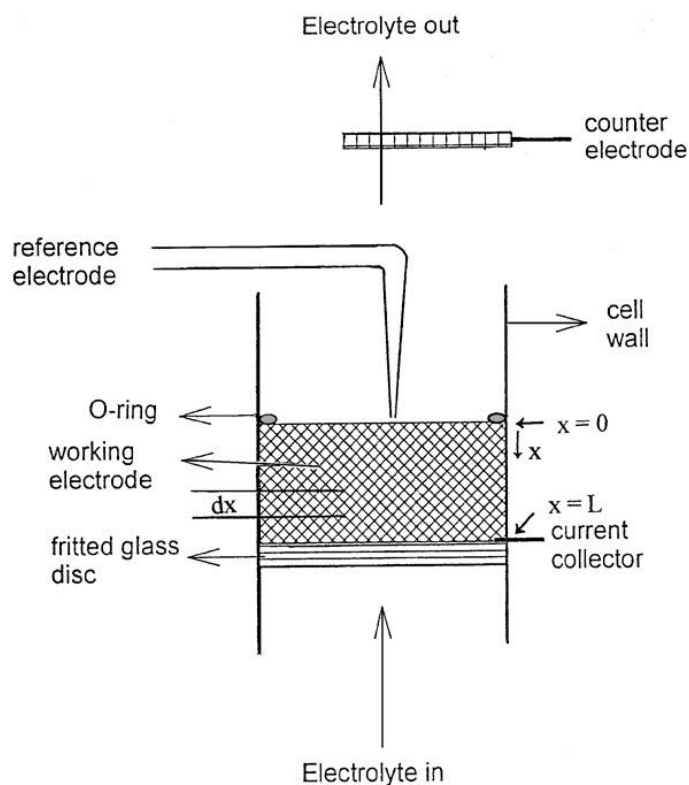


Figure 2. Schematic illustration of the experimental setup of electrolytic cell and the porous electrode chamber.

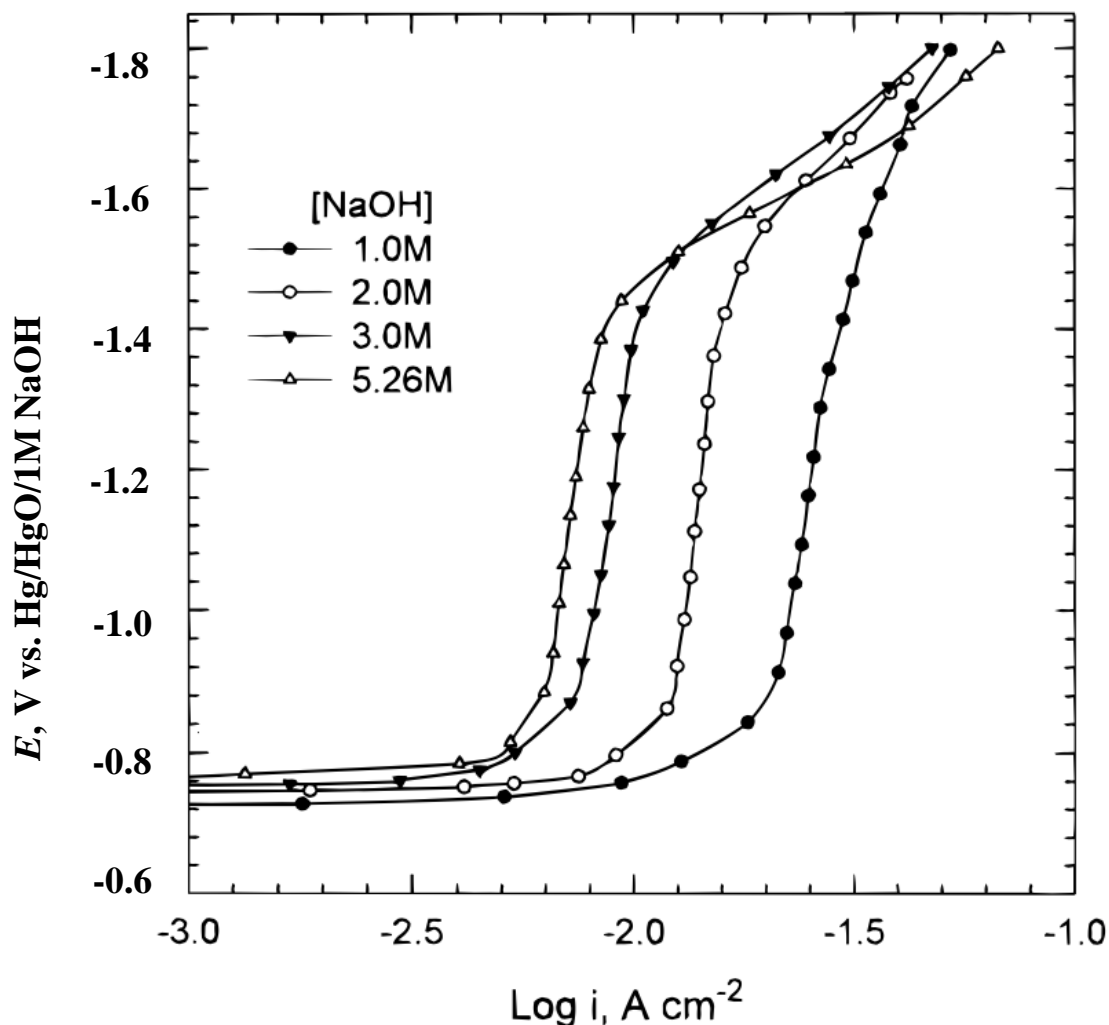


Figure 3. Polarization (i - E) correlation for lead ions deposition onto packed bed porous electrode (composed of 6 stacked screens, mesh size = 60 ppi, thickness = 0.33 cm) from alkaline NaOH solutions containing 40 ppm lead ions flowing at a rate of 1.15 cm s^{-1} .

The diffusion limit of the lead ions deposition reaction is the part at which the limiting current is attained starting from a potential of -0.9 V (vs. Hg/HgO), beyond this potential any increase in cathodic polarization does not increase the measured current until the hydrogen evolution starts to contribute significantly, demonstrated by the inflection point in current observed at around -1.4 V (vs. Hg/HgO).

The effect of pH on the cation complex is a very important point. In such high pH (ca. 14), lead ions exists as plumbite ions PbO_2^{2-} , rather than Pb^{2+} ions (according to Pourbaix diagram). Thus the cathodic reduction (i.e., the electro-deposition) of lead takes place according to the following equation:



Whereas the hydrogen evolution reaction (HER) takes place (as a competing reaction) in alkaline medium according to:



where E_1 and E_2 are the equilibrium potentials for the lead deposition and hydrogen evolution reactions, respectively under the present experimental conditions. The HER current is measured using a blank electrolyte of NaOH in the absence of lead ions. The contribution of the hydrogen evolution reaction currents amounts to ca. 17% of the total measured limiting current density. After each experiment, the packed bed electrode was washed with copious amounts of distilled water, then the screens are dried and weighed. The current distribution of lead ions deposition is determined within the matrix of the porous electrode by weighing each screen of the packed bed before and after the galvanostatic deposition experiment. This procedure is carried out under various operating conditions of electrolyte flow rate, and resistivity as well as various thicknesses of the packed bed porous electrode with an aim to optimize the current distribution for better utilization of the cell house.

3. RESULTS AND DISCUSSION

3.1. Effect of electrolyte resistivity

The effect of electrolyte resistivity on the distribution of the lead ions deposition reaction is studied, i.e., using 1.0 and 3.0 M NaOH solutions containing 10 mM lead ions flowing at a rate (v) of 0.8 cm s^{-1} . Each electrode is composed of 10-stacked screens, having a total thickness of 0.56 cm.

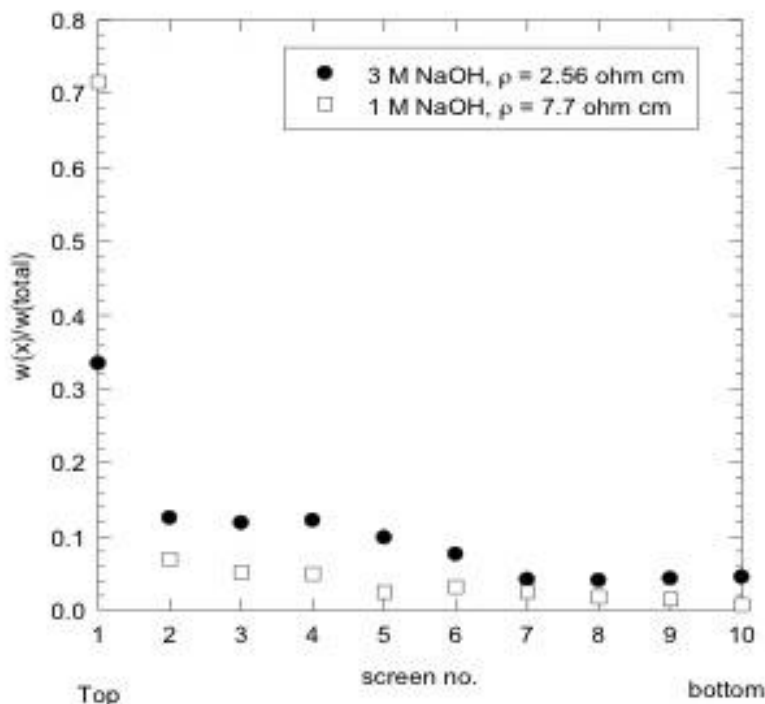


Figure 4. Effect of electrolyte resistivity on the lead current distribution. The electrode was 0.56 cm thick (10 screens of 60 mesh), $v = 0.8 \text{ cm s}^{-1}$, $T = 30^\circ\text{C}$. All electrolytes contained 10 mM lead ions, $i_{\text{cell}} = 200 \text{ mA cm}^{-2}$, $t = 20 \text{ min}$.

The cell current density was 200 mA cm^{-2} . Fig. 4 shows the effect of electrolyte resistivity on the distribution of the lead current after 20 minutes of continuous electrolysis. Note that $w(x)$ refers to the weight gain of each relevant screen composing the packed bed porous electrode, where x refers to the screen number in the stack. And $w(\text{total})$ refers to the total weight of the electrodeposited lead within the porous electrode (i.e., the summation of all $w(x)$). Thus, $w(x)/w(\text{total})$ is the fraction of the total weight of lead at a particular screen in the stack and it is a unitless ratio. The electrodeposition of lead is carried out at a constant current density, thus, the total amount of the electrodeposited lead is assumed constant, albeit with various distribution according to the prevailing experimental conditions. (See Figs. 4 and 5). Fig. 4 reveals the following points:

(i) The distribution of lead ions deposition current from the 1 M NaOH electrolyte (with a specific resistivity $\rho^0 = 7.7 \text{ ohm cm}$) is less uniform than that resulting from the 3 M NaOH electrolyte ($\rho^0 = 2.6 \text{ ohm cm}$).

(ii) Furthermore, the topmost screen supports a larger fraction of the total deposition current in the case of 1 M NaOH than the corresponding screen in the case of 3 M NaOH. It follows that plugging of the topmost screen in the case of the 1 M NaOH (which has a higher resistivity) occurs faster than in the case of the 3 M NaOH (with lower ρ).

(iii) The remaining underlying screens (below the topmost one) support a higher fraction of the total deposited lead in the case of the 3 M NaOH than in the case of the 1 M NaOH, i.e., the uniformity of the reaction is markedly enhanced in 3 M NaOH solution.

This behavior could be reasonably rationalized in view of a dimensionless ohmic index group (Δ), given by [34]:

$$\Delta = i_L \rho_{\text{eff}} L / b \quad (3\text{-a})$$

$$\rho_{\text{eff}} (= \rho^0 [\theta - \varepsilon]^{-1.5}) \quad (3\text{-b})$$

where i_L is the limiting current density, A cm^{-2} , ρ_{eff} is the effective resistivity of the pore electrolyte, ohm cm , of the porous matrix with a porosity (θ) and filled with a fraction of gas bubbles (ε), L is the electrode thickness, cm , and $b = RT/F$, V . Eq. 3 is derived for the case of an electrochemical reaction proceeding with a 100% collection efficiency on an electrode with sufficiently small pore diameter to justify the assumption of one dimensional transport in the axial direction [30]. Similar equations are derived by various authors [33,36-38] using the exchange current density (i_0) instead of i_L . Thus, a similar index, ξ , is developed for the ohmic potential drop within the porous electrode in terms of cell current density (i_{cell}), i.e.

$$\xi = i_{\text{cell}} \rho_{\text{eff}} L / b \quad (4)$$

Accordingly, a decrease of the magnitude of ξ enhances the uniformity of the current distribution, and vice versa. Values of ξ of ca. 34 and 11 are calculated for the 1.0 and 3.0 M NaOH electrolytes, respectively. These values might be much larger if one considers the iR drop caused by the simultaneously electro-generated hydrogen gas bubbles, which increases the void fraction (ε) within the porous matrix filled with insulating gas bubbles. That is Clearly the system with a larger value of ξ (1.0

M NaOH) yields a less uniform current distribution than that of the 3.0 M NaOH (with a lower electrical resistivity). Note that the increase of the NaOH concentration causes also a favorable increase in its viscosity, albeit it lowers the diffusion coefficient of the lead ions. This might be attributed to the effect of electrolyte viscosity on the bubble size of the electro-generated hydrogen gas bubbles down to a favorable level facilitating its sweeping away with the electrolyte flow, thus decreasing the iR contribution within the porous matrix and enhances the current distribution concurrently.

3.2. Effect of electrode thickness

Figs. 5(a-c) shows the effect of the electrode thickness (i.e., number of stacked screens) on the distribution of the lead deposition reaction current from 1.0 M NaOH electrolyte containing 10 mM lead ions flowing at a rate (v) of 0.8 cm s^{-1} . The electrode thickness varied from 0.33 cm (6 stacked screens of 60 mesh) up to 1.1 cm (20 screens of 60 mesh).

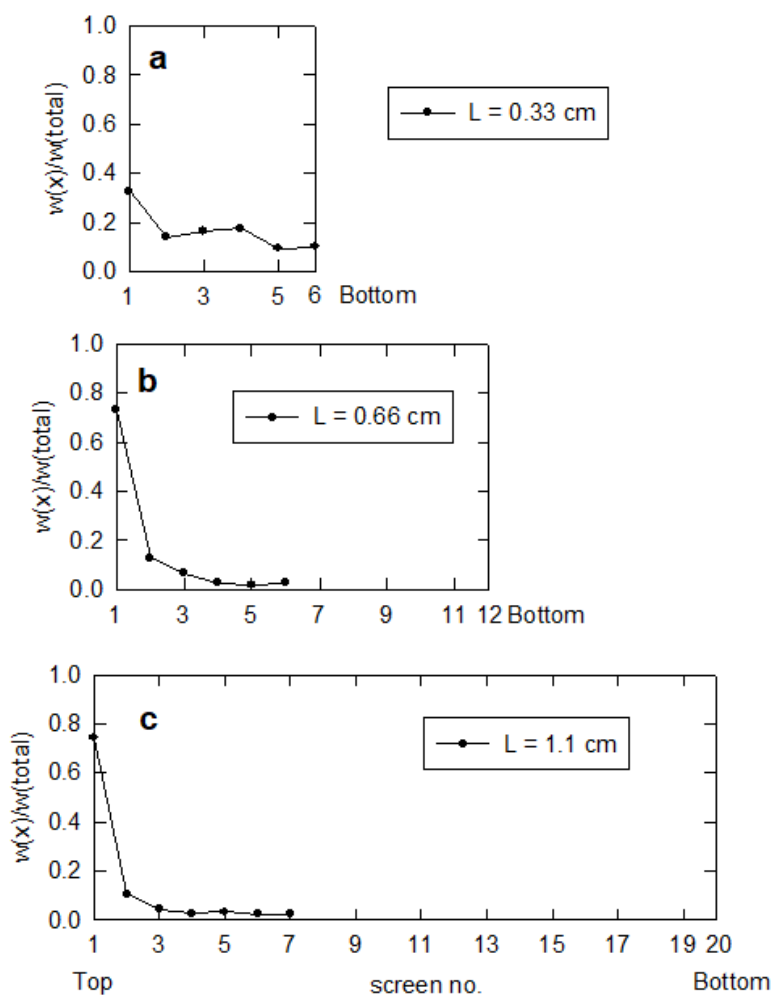


Figure 5. Effect of electrode thickness on the lead current distribution. The electrolyte was 1 M NaOH containing 10 mM lead ions, $v = 0.8 \text{ cm s}^{-1}$, $T = 30^\circ\text{C}$. $i_{\text{cell}} = 200 \text{ mA cm}^{-2}$, $t = 20 \text{ min}$.

The operating conditions have an essential role in determining the fraction of the entire porous packed bed contributing in the reaction. Actually, the experimental conditions are set the same for the

three electrodes (i.e., flow rate, electrolyte concentration, current density, temperature, and deposition time), with the only difference is the electrode thickness. This figure shows obviously that the thicker the electrode, the less uniform current distribution is obtained, i.e., under the prevailing conditions only the top most screens are operable while the underlying ones are not contributing in the overall measured current. That is the fraction of the total lead deposition current supported by the topmost screen increases from ca. 35%, 72% and 75% for electrodes composed of 6 ($L = 0.33$ cm), 12 ($L = 0.66$ cm) and 20 screens ($L = 1.10$ cm), respectively. Whereas, the underlying screens support remaining lesser fractions of the lead deposition current. The thinnest porous electrode (composed of 6 stacked screens, $L = 0.33$ cm) shows a much more uniform current distribution over the remaining underlying 5 screens than those shown by the thicker electrodes over the remaining 11 or 19 screens, i.e., the thinner electrode shows more non-uniform distribution of lead deposition across its entire thickness. On the other hand, the electrode composed of 12 screens ($L = 0.66$ cm) shows a significant weight gain only at the top 4 screens ($\approx 34\%$ of the entire thickness), while the rest of the electrode ($\approx 66\%$) is much underutilized. The non-uniformity is signified for the thick electrode where only 25% of the entire thick is in operation (albeit ill-distributed current) and the rest of the electrode (75% of its thickness) is much underutilized under the same operating conditions. This could be reasonably explained in view of the variation of the ohmic index, ξ (Eq. 4), with the electrode thickness, for the conditions under which the above distributions are measured. Using a value of current of $i_{\text{cell}} = 200 \text{ mA cm}^{-2}$, a resistivity of 7.7 ohm cm for the 1.0 M NaOH electrolyte and values of thicknesses of 0.33, 0.66 and 1.10 cm (6, 12 and 20 screens of 60 mesh), values of ξ of ca. 20, 40 and 66 are calculated for the current distributions shown in Fig. 5(a-c), which is in line with the increasing non-uniformity of the lead deposition current.

3.3. Effect of electrolyte flow rate

Fig. 6 shows the effect of the electrolyte flow rate (v) on the distribution of the lead deposition reaction current within the matrix of a porous electrode made up of 10 stacked screens of 60 mesh ($L = 0.56$ cm) from 3.0 M NaOH containing 10 mM lead ions flowing at 0.2 and 0.8 cm s^{-1} . This figure shows that the increase of the electrolyte flow rate (v) is associated with a considerable improvement of the uniformity of the lead deposition reaction, i.e., a larger fraction of the electrode thickness is being utilized to support the reaction at relatively higher flow rate. It worthy to mention here that two competing cathodic reactions account for the total measured current, i_{total} , supported by the lead-containing electrolyte, i.e., lead ions deposition and HER (see Eqs. 1 and 2 above). The coulombic efficiency of the lead deposition reaction is estimated by comparing the experimentally obtained total weight of the electrodeposited lead ions with the predicted value applying Faraday's law. A current efficiency for lead deposition amounts to ca. 83%, while the remaining 17% are consumed in the HER, thus, indispensable amount of hydrogen gas bubbles are generated concurrently with lead ions deposition. Consequently, the observed behavior (in Fig. 6) could be reasonably attributed to the mechanical sweeping of the hydrogen gas bubbles (locally generated within the porous matrix) by the forced convection of the electrolyte flow, which sweeps the simultaneously generated gas bubbles. This leads to a decrease of gas void fraction (ϵ), and consequently the pore electrolyte resistivity and the ohmic

potential drop within the electrode [6,36, 46, 47]. The effect of gas bubbles was expressed in terms of a bubble group, Γ , given by [6,36, 46, 47]:

$$\Gamma = 2PFv/i_{cell} RT \quad (5)$$

This dimensionless group, Γ , measures the ratio of the electrolyte flow rate, v , to the rate of generation of hydrogen gas bubbles at a cell current density, i_{cell} . Small values of Γ indicate more predominant bubble effects and hence larger ohmic potential drop, ξ , and less uniform current distributions [32]. This is obtained under conditions of high cell currents and/or low electrolyte flow rates. Thus, the increase of electrolyte flow rate would enhance the uniformity of the lead current distribution.

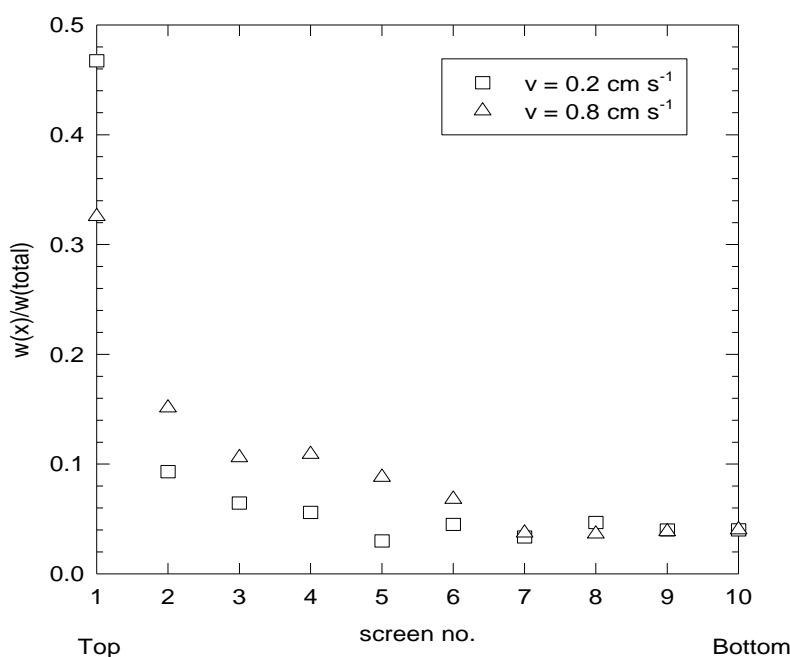


Figure 6. Effect of electrolyte flow rate on the lead current distribution. The electrode was 0.56 cm thick (10 screens of 60 mesh), $T = 30^\circ\text{C}$. The electrolyte is 3 M NaOH containing 10 mM lead, $i_{cell} = 200 \text{ mA cm}^{-2}$, $t = 20 \text{ min}$.

4. CONCLUSIONS

In this study, the effects of electrolyte resistivity and flow rate and the electrode thickness on the current distribution of the lead deposition reaction within PFTE are addressed. The current distribution is generally non-uniform. The uniformity of the current distribution increases (i.e., increased utilization of the porous electrode cell house) with the decrease of electrolyte resistivity and/or increase of flow rate. On the other hand, the increase of the electrode thickness resulted in a more non-uniform distribution of the current. This behavior is explained on the basis of the ohmic potential drop index (ξ) within the pore electrolyte and the effect of the simultaneously electro-generated hydrogen gas bubbles within the porous matrix. Increases of the electrode thickness and/or electrolyte resistivity (with a

decrease of electrolyte flow rate) leads to a corresponding increase of ξ and thus less uniform current distribution is expected and vice versa.

References

1. M. R. Rizk, M. G. Abd El-Moghny, M. S. El-Deab, *J. Electrochem. Soc.*, 167 (2020) 114505.
2. D. M. Sayed, M. S. El-Deab, N. K. Allam, *Separation and Purification Technology*, 266 (2021) 118597.
3. J. S. Shahat, M. I. Balaha, M. S. El-Deab, A. M. Attia, *Energy Reports*, 7 (2021) 711-723.
4. M. S. El-Deab, M. M. Saleh, B. E. El-Anadouli, B. G. Ateya, *J. Electrochem. Soc.*, 146 (1999) 208-213.
5. M. S. El-Deab, M. E. El-Shakre, B. E. El-Anadouli, B. G. Ateya, *Int. J. Hydrogen Energy*, 21 (1996) 273-280.
6. M. M. Saleh, *J. Phys. Chem. B*, 108 (2004) 13419-13426.
7. A. M. Abdelrahim, M. G. Abd El-Moghny, M. E. El-Shakre, M. S. El-Deab, *Electrochim. Acta*, 378 (2021) 137991.
8. M. S. El-Deab, F. Kitamura, T. Ohsaka, *J. Electrochem. Soc.*, 160(6) (2013) F651-F658.
9. X. Shi, Y. Shuai, F. Wang, C. Zhang, Z. Cheng, X. Chen, *J. CO₂ Utilization*, 37 (2020) 147-157.
10. M. Mottaghi, S. Kuhn, *Chem. Eng. Sci.* 208 (2019) 115146.
11. Y. Wang, D. Sun, T. Chowdhury, J. S. Wagner, T. J. Kempa, and A. S. Hall, *J. Am. Chem. Soc.*, 141 (2019) 2342.
12. Y. Wang, and A. S. Hall, *ACS Energy Lett.*, 5 (2020) 17.
13. W. Luo, J. Zhang, M. Li, and A. Zuttel, *ACS Catal.*, 9 (2019) 3783.
14. A. Varzi, L. Mattarozzi, S. Cattarin, P. Guerriero, and S. Passerini, *Adv. Energy Mat.*, 8(1) (2018) 1701706.
15. M. S. Wu, Y. J. Sie, and S. B. Yang, *Electrochim. Acta*, 304 (2019)131–137.
16. A. Ashok, A. Kumar, J. Ponraj, S. A. Mansour, and F. Tarlochan, *J. Electrochem. Soc.*, 165, J3301–J3309 (2018).
17. M. R. Rizk, M. G. Abd El-Moghny, A. Mazhar, M. S. El-Deab, B. E. El-Anadouli, *Sustainable Energy & Fuels*, 5(4) (2021) 986-994.
18. M. S. El-Deab, M. M. Saleh, *Int. J. Hydrogen Energy*, 28 (2003) 1199-1206.
19. M. M. Saleh, C. Weidlich, K.-M. Mangold, K. Juttner, *J. Appl. Electrochem.*, 36 (2006) 179-186.
20. M. M. Saleh, *J. Appl. Electrochem.*, 30 (2000) 939-944.
21. M. M. Saleh, M. H. El-Ankily, M. S. El-Deab, B. E. El-Anadouli, *Bull. Chem. Soc. Japan*, 79 (2006) 1711-1718.
22. P. W. A. M. Wenmakers, J. van der Schaaf, B. F. Kuster, J. C. Schouten, *Chem. Eng. Sci.*, 65 (2010) 147-254.
23. W. Zhou, L. Rajic, Y. Zhao, J. Gao, Y. Qin, A. N. Alshawabkeh, *Electrochim. Acta*, 277 (2018) 185-196.
24. G. Ramírez, F. J. Recio, P. Hírrasti, C. P.-de-Leon, I. Sirés, *Electrochim. Acta* 204 (2016) 9-17.
25. M. M. Saleh, J. W. Weidner, B. G. Ateya, *J. Electrochem. Soc.*, 142 (1995) 4113-4121.
26. M. M. Saleh, J. W. Weidner, B. E. El-Anadouli, B. G. Ateya, *J. Electrochem. Soc.*, 142 (1995) 4122-4128.
27. R. de Levie, in *"Advances in Electrochemistry and Electrochemical Engineering"* Vol. 6, P. Delahy Ed., Interscience, New York (1967).
28. J. Newman and W. Tiedman, *"Advances in Electrochemistry and Electrochemical Engineering"* Vol. 11, p. 352, H. Gerischer and C. W. Tobias Eds., John Wiley & Sons, New York (1976).
29. R. E. Sioda and K. B. Keating *"Electroanalytical Chemistry"*, Vol. 12, A. J. Bard Editor, Dekker, New York (1982).

30. F. Goodridge and A. R. Wright, "Porous Flow-Through and Fluidized Bed Electrodes" in "Comprehensive Treatise of Electrochemistry" Vol. 6 Electrochemical processing, J. Bockris, B. E. Conway, E. Yeager and R. E. White Eds., Plenum Press, New York, Chap. 6 (1984).
31. N. A. Hampson and A. J. S. McNeil, "The Electrochemistry of Porous Electrodes, Flow-Through and Three Phase Electrodes", "Electrochemistry", Vol. 9 The Royal Society of Chemistry, London, p. 1-65 (1984).
32. J. Newman, "Electrochemical Systems", 2nd Edn., Chap. 22, Prentice-Hall, Englewood Cliffs, NJ (1991).
33. R. Alkire and B. Gracon, *J. Electrochem. Soc.*, 122 (1975) 1594.
34. B. G. Ateya and L. G. Austin, *J. Electrochem. Soc.*, 124 (1977) 83; B. G. Ateya, L. G. Austin, *J. Electrochem. Soc.*, 124 (1977) 1540.
35. J. A. Trainham and J. Newman, *J. Electrochem. Soc.*, 124 (1977) 1528.
36. B. G. Ateya and B. E. El-Anadouli, *J. Electrochem. Soc.*, 138 (1991) 1331; B. E. El-Anadouli and B. G. Ateya, *J. Appl. Electrochem.*, 22 (1992) 277.
37. M. E. El-Shakre, M. M. Saleh, B. E. El-Anadouli, B. G. Ateya, *J. Electrochem. Soc.*, 141 (1994) 441.
38. K. Kinoshita and S. C. Leach, *J. Electrochem. Soc.*, 129 (1982) 1993.
39. D. T. Chin and B. Eckert, *Plat. Surf. Finish.*, 10 (1976) 38.
40. C. S. Hofseth and T. W. Chapman, *J. Electrochem. Soc.*, 146 (1999) 199.
41. P. M. Lessner, F. R. McLarnon, J. Winnik and E. J. Cairns, *J. Appl. Electrochem.*, 22 (1992) 927.
42. M. Warshy and L. O. Wright, *J. Electrochem. Soc.*, 124 (1977) 173.
43. J. M. Bisang, *J. Appl. Electrochem.*, 26 (1996) 135.
44. E. J. Podlaha and J. M. Fenton, *J. Appl. Electrochem.*, 25 (1995) 29.
45. M. Matlosz and J. Newman, *J. Electrochem. Soc.*, 133 (1986) 1850.
46. M. M. Saleh, M. I. Awad, F. Kitamura, and T. Ohsaka, *Electrochim. Acta*, 51 (2006) 6331.
47. M. M. Saleh, *J. Solid State Electrochem.*, 13 (2009) 343.

© 2021 The Authors. Published by ESG (www.electrochemsci.org). This article is an open access article distributed under the terms and conditions of the Creative Commons Attribution license (<http://creativecommons.org/licenses/by/4.0/>).